ELSEVIER

1 August 1999

Optics Communications 166 (1999) 189–198

OPTICS COMMUNICATIONS

www.elsevier.com/locate/optcom

Full length article

Linear algorithms for stretched exponential decay analysis

Eugene G. Novikov [a,*], Arie van Hoek [b], Antonie J.W.G. Visser [b], Johannes W. Hofstraat [c]

[a] *Systems Analysis Department, Belarusian State University, F. Skarina's avenue 4, Minsk 220050, Belarus*
[b] *MicroSpectroscopy Centre, Department of Biomolecular Sciences, Wageningen Agricultural University, P.O. Box 8128, NL-6700 ET Wageningen, Netherlands*
[c] *Akzo Nobel Central Research, Department RGL, P.O. Box 9300, NL-6800 SB Arnhem, Netherlands*

Received 16 December 1998; received in revised form 29 March 1999; accepted 25 May 1999

Abstract

Several non-iterative algorithms for the analysis of stretched exponential decay are proposed. Decay parameters are obtained by standard linear optimization methods, providing reasonable accuracy, high speed of processing and independence of the initial guesses. The latter feature ensures an excellent possibility to use them for generating initial guesses for iterative procedures, rendering the minimum search more reliable and faster. Proposed algorithms were investigated by fitting simulated data and then used for the analysis of fluorescence and anisotropy decays of dimethylaminonitrostilbene molecules dissolved in polymethyl methacrylate films. © 1999 Published by Elsevier Science B.V. All rights reserved.

Keywords: Stretched exponentials; Linearization; Initial guesses; Fluorescence decay; Anisotropy decay

1. Introduction

The evolution of electronic energy relaxation, taking place after a short impulse of optical excitation, provides important information about the structure, dynamics and photophysical properties of supramolecular structures containing chromophoric molecules. One of the most powerful techniques for the investigation of relaxation processes is the time-correlated single photon counting (TCSPC) method [1,2], where the fluorescence intensity decay of the fluorophore is analyzed in terms of a presumed theoretical decay law. Numerous investigations [3–5] have shown that adequate models for electronic energy relaxation in macromolecules cannot be defined by the commonly used sum of exponentials, when a mechanism of dipole–dipole energy transfer is taken into account. In recent years, most attention has been given to the stretched-exponential Förster decay law [4,6], representing the first-order approximation of dipole–dipole electronic energy transfer. Previous experience [7] indicates that stretched exponential decay fitting is more difficult than the usual multi-exponential analysis. An important problem is related to the influence of the initial guesses on the efficiency of fit. Commonly used iterative fitting

* Corresponding author. Present address: Department of Chemistry, K.U. Leuven, Celestijnlaan 200F, 3001 Heverlee, Belgium. E-mail: Eugene.Novikov@chem.kuleuven.ac.be

PII: S0030-4018(99)00262-X

methods only work well when the initial guesses are chosen close to the true values of parameters.

This paper proposes several non-iterative algorithms for the analysis of stretched exponential decay. Decay parameters are obtained by standard methods of linear optimization, providing reasonable accuracy, high speed of processing and independence of the initial guesses. The latter feature enables to use them for generating initial guesses for iterative procedures, rendering the minimum search more reliable and faster.

2. Stretched exponential decay

When the concentration of donor molecules is sufficiently low, such that the probability of multistage energy migration processes is negligible and energy is directly transferred to the random distribution of acceptors, the donor fluorescence decay can be represented by a stretched exponential [4]:

$$I(t) = I_0 \exp\{-\lambda t - \gamma t^{\delta}\}, \tag{1}$$

where $\lambda = 1/\beta$ (β is the donor lifetime), $\gamma = C/\beta^{\delta}$ (C is the parameter characterizing the amount of energy transfer [4]), I_0 is the intensity at zero time ($t = 0$) and δ is determined by the geometrical dimension d of a sample as $\delta = d/6$ (for two dimensions $\delta = 1/3$, for three dimensions $\delta = 1/2$). Special attention is attracted by samples with a so-called fractal (non-integer) dimension [8]. In the latter case, a theoretical calculation of the dimensional parameter δ is not straightforward, and often requires approximation.

If the dimensional parameter δ in Eq. (1) is known exactly, the estimation of the other parameters (I_0, λ and γ) can be done after the transformation of the stretched exponential Eq. (1) to a differential equation, which is linear with respect to the unknown parameters [9]:

$$I'(t) = -\lambda I(t) - \gamma\delta t^{\delta-1} I(t), \tag{2}$$

with the initial condition $I(0) = I_0$. Statistical distortions of the data, collected in $I(t)$, are smoothed by integrating Eq. (2):

$$I(t) = -\lambda \int_0^t I(x)\,\mathrm{d}x - \gamma\delta \int_0^t x^{\delta-1} I(x)\,\mathrm{d}x + I_0. \tag{3}$$

Application of the standard linear least squares method [10] to the last equation yields:

$$\sum_{i=1}^{N} \omega(t_i) \left\{ I(t_i) + \lambda \int_0^{t_i} I(x)\,\mathrm{d}x + \gamma\delta \int_0^{t_i} x^{\delta-1} I(x)\,\mathrm{d}x - I_0 \right\}^2 = \min, \tag{4}$$

where $\omega(t_i)$ is the weight factor, equal to $1/I(t_i)$, for the Poisson statistics of collected counts, and N is the number of time channels.

The right part of Eq. (3) contains the component $x^{\delta-1}$, which becomes infinite when $x = 0$ and $\delta < 1$. To avoid the problems of numerical implementation arising in that case, integration should be done with a special multiplication factor $w(x)$:

$$w(t)\,I(t) - \int_0^t w'(x)\,I(x)\,\mathrm{d}x = -\lambda \int_0^t w(x)\,I(x)\,\mathrm{d}x - \gamma\delta \int_0^t w(x)\,x^{\delta-1} I(x)\,\mathrm{d}x. \tag{5}$$

If, for instance, $w(t) = t$, Eq. (5) takes the form:

$$tI(t) - \int_0^t I(x)\,\mathrm{d}x = -\lambda \int_0^t xI(x)\,\mathrm{d}x - \gamma\delta \int_0^t x^{\delta} I(x)\,\mathrm{d}x, \tag{6}$$

in which the infinity component is eliminated. Moreover, the integration with the multiplication factor has removed the amplitude I_0 from the last equation. The amplitude is often only a scaling factor and not really important. If, however, the amplitude I_0 is required, the linear least-squares method can be applied directly to Eq. (1), when parameters λ are γ have been already defined according to Eq. (6). The methods of error propagation [10] lead to the following expression for the statistical weight in the linear least squares method: $\omega(t) = 1/(t^2 I(t))$, where statistical noise of the integrals is ignored.

Eqs. (3), (4) and (6) can be readily adopted for the analysis of decays with an additive background: $I^b(t) = I(t) + B$, where B is the intensity of background radiation. From Eq. (6) one obtains:

$$tI^b(t) - \int_0^t I^b(x)\,dx = -\lambda\int_0^t xI^b(x)\,dx - \gamma\delta\int_0^t x^\delta I^b(x)\,dx - \lambda Bt^2/2 - \gamma B\delta t^{\delta+1}/(\delta+1), \quad (7)$$

and the parameters of the stretched exponential decay as well as the intensity of background can be found by the linear least squares method.

The above considerations are valid, when the dimensional parameter δ is known. If it must be estimated, linearization of Eq. (1) with respect to δ can be done in two ways. Both of them use the logarithm of $I(t)$:

$$\log(I(t)) = \log(I_0) - \lambda t - \gamma t^\delta. \quad (8)$$

The idea consist of the elimination of the factor t^δ from the final expressions. Combining Eqs. (2) and (8) yields:

$$tI(t) = \delta\int_0^t I(x)\log(I(x))\,dx - [\delta\log(I_0) - 1]\int_0^t I(x)\,dx + \lambda(\delta-1)\int_0^t xI(x)\,dx. \quad (9)$$

Another transformation is done via the differentiation of Eq. (8) with respect to t:

$$[\log(I(t))]' = -\lambda - \delta\gamma t^{\delta-1}. \quad (10)$$

Substituting Eq. (10) into Eq. (8) gives the equation:

$$t\log(I(t)) = (1+\delta)\int_0^t \log(I(x))\,dx - \delta\log(I_0)t + \lambda(\delta-1)t^2/2. \quad (11)$$

Eqs. (9) and (11) are linear and allow to estimate the dimensional parameter δ, lifetime β and initial intensity I_0 by standard means of linear optimization. The amount of energy transfer C can be directly derived from Eq. (4) or Eq. (6), when the dimensional parameter δ has previously been estimated.

3. Additional exponential term

Several modifications of the basic stretched exponential decay law Eq. (1) were proposed [4,11]. Heterogeneity in chromophore surroundings or processes such as excimer formation lead to the appearance of additional components in the fluorescence decay of the investigated samples. In the simplest case, one extra exponential term with the same decay parameter λ may be considered:

$$I(t) = I_0\exp\{-\lambda t - \gamma t^\delta\} + A\exp\{-\lambda t\}, \quad (12)$$

where A is the amplitude of the second component. The extra component can be explained by a non-homogeneous distribution of acceptors, resulting in the appearance of isolated donor molecules [4,11]. In this section, we assume that the dimensional parameter δ is known exactly and fixed. It can be shown that Eq. (12) is the solution of the following linear differential equation:

$$I''(t) = I'(t)\left[(\delta-1)t^{-1} - 2\lambda - \gamma\delta t^{\delta-1}\right] + I(t)\left[\lambda t^{-1}(\delta-1) - \gamma\delta\lambda t^{\delta-1} - \lambda^2\right], \quad (13)$$

with the initial conditions $I(0) = I_0 + A$ and $I'(0) = 0$. Integrating Eq. (13) twice with the multiplication factor $w(t) = t$ yields:

$$F(\gamma,\lambda,t) = \phi(t) + \lambda s_0(t) + \gamma\lambda s_1(t) + \gamma s_2(t) + \lambda^2 s_3(t) = 0, \quad (14)$$

where

$$\phi(t) = -\left[(\delta+3)\int_0^t xI(x)\,dx - (\delta+1)\int_0^t (t-x)I(x)\,dx - t^2 I(t)\right];$$

$$s_0(t) = -\left[(\delta+3)\int_0^t x(t-x)I(x)\,dx - 2\int_0^t x^2 I(x)\,dx\right];$$

$$s_1(t) = -\delta\int_0^t x^{\delta+1}(t-x)I(x)\,dx;$$

$$s_2(t) = -\delta\left[\int_0^t x^{\delta+1}I(x)\,dx - (\delta+1)\int_0^t x^\delta(t-x)I(x)\,dx\right];$$

$$s_3(t) = -\int_0^t x^2(t-x)I(x)\,dx. \quad (15)$$

Eq. (14) is linear with respect to the parameters λ, γ, $\gamma\lambda$ and λ^2, which can be, for example, obtained by the linear least squares method. Amplitude parameters can be easily evaluated, applying the least squares procedure to the primary Eq. (12), when parameters λ and γ are already known. A significant drawback of this approach is that it is necessary to fit four coefficients of the linear Eq. (14), while one has only two unknown parameters λ and γ. An artificially extended set of unknown parameters (four instead of two) requires an increase of the dimension of the set of normal equations (up to four) in the method of least squares. Usually this causes extra distortions in solution.

An alternative approach is to consider Eq. (14) as a nonlinear functional equation with respect to two unknowns, γ and λ. Then, minimization of Eq. (14) gives a set of two non-linear algebraic equations:

$$F(\gamma,\lambda,t)\{s_0(t)+\gamma s_1(t)+2\lambda s_3(t)\}=0,$$

$$F(\gamma,\lambda,t)\{\lambda s_1(t)+s_2(t)\}=0. \quad (16)$$

The dimension of the set in Eq. (16) is small and can easily be solved analytically. Testing has shown that the latter approach ensures a higher accuracy of solution compared to the first one and it can be considered as a method of choice in the analysis of stretched exponential decay with the added exponential term.

4. Anisotropy

Important information about energy migration can be retrieved from fluorescence depolarization measurements: the detected fluorescence anisotropy depends on two main sources of depolarization, namely excitation transfer and chromophore rotation. Let us consider the case where molecules are motionless during the time scale of a fluorescence decay experiment (for instance in solid solutions, e.g. polymers), and the time dependence of the fluorescence anisotropy is exclusively determined by the process of energy transfer. The anisotropy decay for donor–donor energy transfer takes the following form [12]:

$$r(t)=r_0\exp\{-\gamma t^{\delta}\}, \quad (17)$$

where $\gamma=C/\beta^{\delta}$ and r_0 is the limiting anisotropy (at $t=0$). It was shown [13] that the function $\exp\{-\gamma t^{\delta}\}$ contains all information about energy transfer that influences the anisotropy decay. If the transition dipole distribution is not random, the following model for the anisotropy decay can be used:

$$r(t)=a_1\exp\{-\gamma t^{\delta}\}+a_2, \quad (18)$$

where a_1 represents the amplitude of the energy transfer component and a_2 is a constant, time-independent component, which is due to, for example, the nonrandom distribution of transition dipoles. Analysis of the anisotropy decays can be performed in the same way as for the fluorescence decay. For example, application of the functional Eq. (7) to the model, given by Eq. (18), yields:

$$tr(t)-\int_0^t r(x)\,dx=-\gamma\delta\int_0^t x^{\delta}r(x)\,dx - \gamma a_2\,\delta t^{\delta+1}/(\delta+1), \quad (19)$$

and anisotropy parameters γ and a_2 can be readily recovered. The amplitude of the stretched exponential a_1 can be obtained afterwards by application of the least squares method directly to Eq. (18).

5. Deconvolution

The observed experimental decay curves only correspond to the true ones when the light source produces infinitely narrow excitation pulses and when the response of the detection system is ultrafast. In practice the detected fluorescence intensity f(t) is represented by a convolution of the true decay function with the instrumental response function $g(t)$ [14]:

$$f(t)=\int_0^t I(t-x)\,g(x)\,dx. \quad (20)$$

It appeared not to be possible to find a direct transformation of the convoluted stretched exponential decay curve to the functional equation, linear with respect to the unknown parameters, as it is possible for multi-exponential [15] or unconvoluted stretched exponential decays.

An alternative approach consists of the preliminary non-parametric deconvolution of Eq. (20), thus

getting undistorted fluorescence decay $I(t)$, which can subsequently be fitted by the derived algorithms. Numerous deconvolution routines are known. Among them, probably the most appropriate one is based on the approximation of the stretch exponential decay curve by a sum of exponentials [16]:

$$I(t) \approx \sum_{i=1}^{n} A_i \exp(-t/\tau_i), \quad (21)$$

where A_i are the amplitudes of exponentials, τ_i are the decay times and n is the number of exponentials. The decay times in Eq. (21) can be variable or fixed. One usually needs up to four exponentials, when the decay times are variable, and up to ten when they are fixed. The set of parameters A_i and τ_i can be recovered by one of the common techniques for multi-exponential fitting [1,2]. These parameters then can be used to generate the unconvoluted profile, from which parameters of the stretched exponential decay are evaluated. In this approach, the multi-exponential decay is used only for the approximation, and the obtained parameters A_i and τ_i do not contain any physical meaning.

In the time-resolved method of anisotropy measurements, the fluorescence intensity profiles for parallel $f_{\parallel}(t)$ and perpendicular $f_{\perp}(t)$ components of emitted light are detected. These components are related to the true functions of fluorescence and anisotropy as [14]:

$$f_{\parallel}(t) = \int_0^t I(t-x)\left[1 + 2r(t-x)\right] g(x)\,\mathrm{d}x, \quad (22)$$

$$f_{\perp}(t) = \int_0^t I(t-x)\left[1 - r(t-x)\right] g(x)\,\mathrm{d}x. \quad (23)$$

It is clear that in this situation direct application of the linear algorithms for the analysis of the anisotropy $r(t)$ and fluorescence $I(t)$ decays, represented by stretched exponential functions, is impossible. Analysis should be performed in several steps. First, the true fluorescence decay $I(t)$, approximated by Eq. (21), can be deconvoluted from the total fluorescence profile of Eq. (20) and then fitted. The anisotropy decay $r(t)$ can also be approximated by a sum of exponentials, parameters of which can be obtained by simultaneous analysis of the parallel (Eq. (22)) and perpendicular (Eq. (23)) polarized components of fluorescence [17]. The application of the linear

Table 1
Estimation of the parameters of stretch exponential decay (Eq. (1)) from simulated data

δ	Method	Estimator	Without instrumental response			With instrumental response		
			$\beta = 8.0$	$C = 1.0$	δ^*	$\beta = 8.0$	$C = 1.0$	δ^*
0.75	Linear	M	7.99	1.00	0.73	7.97	0.99	0.74
		σ	0.29	0.072	0.040	0.17	0.041	0.055
	MNLLS	M	7.97	1.00	0.74	7.99	0.99	0.75
		σ	0.18	0.046	0.030	0.15	0.037	0.026
0.5	Linear	M	8.03	1.01	0.49	8.05	1.02	0.51
		σ	0.13	0.043	0.020	0.074	0.019	0.026
	MNLLS	M	7.98	0.99	0.49	7.99	1.00	0.49
		σ	0.078	0.021	0.012	0.063	0.017	0.013
1/3	Linear	M	8.04	1.03	0.31	8.13	1.05	0.34
		σ	0.091	0.029	0.016	0.052	0.016	0.021
	MNLLS	M	7.97	0.99	0.33	8.00	1.00	0.33
		σ	0.050	0.016	0.0073	0.041	0.013	0.0091
1/6	Linear	M	8.21	1.15	0.093	8.30	1.20	0.15
		σ	0.071	0.038	0.017	0.039	0.019	0.022
	MNLLS	M	7.98	0.99	0.17	7.99	0.99	0.16
		σ	0.031	0.014	0.0032	0.027	0.013	0.0061

Number of channels is 256, width of a channel is 0.1 (*: 1024 channels, width of a channel 0.025). Peak count 10^4.

Table 2
Estimation of the parameters of stretch exponential decay (Eq. (12)) from simulated data

δ	Method	Estimator	Without instrumental response				With instrumental response			
			$I_0 = 2.0$	$\beta = 8.0$	$C = 3.0$	$A = 1.0$	$I_0 = 2.0$	$\beta = 8.0$	$C = 3.0$	$A = 1.0$
0.75	Linear	M	2.00	8.00	3.00	1.00	2.00	7.99	3.01	1.00
		σ	0.020	0.066	0.055	0.019	0.016	0.057	0.044	0.015
	MNLLS	M	2.00	7.99	2.99	1.00	2.00	7.99	2.99	1.00
		σ	0.018	0.063	0.045	0.017	0.013	0.052	0.041	0.013
0.5	Linear	M	2.03	7.96	3.10	1.02	2.06	7.93	3.16	1.03
		σ	0.033	0.071	0.11	0.024	0.027	0.054	0.082	0.017
	MNLLS	M	2.00	7.98	3.00	1.00	2.01	7.99	3.00	0.99
		σ	0.023	0.066	0.072	0.019	0.019	0.051	0.077	0.014
1/3	Linear	M	2.28	8.03	3.45	1.03	2.17	7.82	3.26	1.08
		σ	0.16	1.13	0.32	0.17	0.095	0.043	0.16	0.015
	MNLLS	M	2.01	7.98	3.00	0.99	2.01	8.00	3.00	1.01
		σ	0.029	0.058	0.090	0.018	0.038	0.040	0.12	0.010
1/6*	Linear	M	2.15	8.01	3.09	0.99	2.32	7.94	3.18	1.05
		σ	0.30	0.052	0.41	0.041	0.31	0.026	0.26	0.014
	MNLLS	M	1.99	7.99	2.99	1.01	2.00	8.00	3.00	1.01
		σ	0.025	0.021	0.056	0.0093	0.080	0.021	0.13	0.013

Number of channels is 256, width of a channel is 0.1 (*: 1024 channels, width of a channel 0.025). Peak count 10^4.

algorithms for stretched exponential decay analysis of $r(t)$ is then straightforward (see Section 4).

6. Simulated data

The proposed algorithms were implemented and thoroughly tested via simulations. We use the following representation for the instrumental response $g(t)$ [1]:

$$g(t) = \exp(-t/0.6) - \exp(t/1.1). \quad (24)$$

All values here and further are given in relative units. The number of time channels is 256 (the width of a channel is 0.1) or 1024 (the width of a channel

Table 3
Estimation of the parameters of stretch exponential decay (Eq. (18)) from simulated data

δ	Method	Estimator	With constant anisotropy			Without constant anisotropy		
			$a_1 = 0.3$	$C = 2.0$	$a_2 = 0.1$	$a_1 = 0.3$	$C = 2.0$	$a_2 = 0.0$
0.75	Linear	M	0.29	1.91	0.098	0.30	2.06	0.00
		σ	0.0082	0.17	0.0041	0.0090	0.14	0.0023
	MNLLS	M	0.30	1.99	0.099	0.30	1.99	0.0002
		σ	0.0036	0.066	0.0021	0.0032	0.059	0.0018
0.5	Linear	M	0.29	1.90	0.096	0.30	1.99	0.00
		σ	0.012	0.25	0.0073	0.013	0.20	0.0043
	MNLLS	M	0.30	1.99	0.098	0.30	1.99	0.0006
		σ	0.0058	0.092	0.0029	0.0052	0.082	0.0026
1/3	Linear	M	0.30	1.92	0.092	0.29	1.90	0.010
		σ	0.019	0.42	0.016	0.022	0.43	0.014
	MNLLS	M	0.30	1.98	0.098	0.30	1.98	0.0021
		σ	0.0099	0.14	0.0044	0.0088	0.12	0.0039
1/6	Linear	M	0.32	2.29	0.092	0.35	2.18	0.017
		σ	0.064	0.94	0.062	0.22	1.03	0.098
	MNLLS	M	0.31	1.96	0.096	0.30	1.95	0.0040
		σ	0.018	0.23	0.0082	0.015	0.21	0.0073

Number of channels is 256, width of a channel is 0.1. Fluorescence lifetime β is 5. Peak count 10^4.

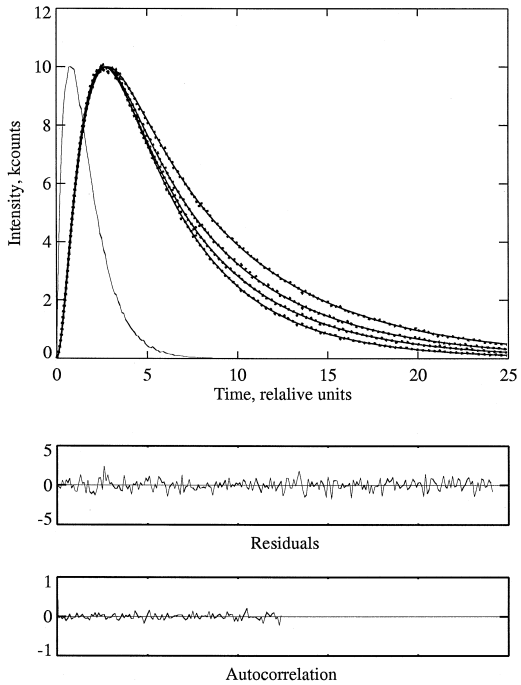

Fig. 1. Simulated (dots) and fitted (smooth curve) fluorescence stretched exponential decay (Eq. (1)) for four values of the dimensional parameter δ: 0.75 (the longest decay), $1/2$, $1/3$ and $1/6$ (the shortest decay). Residuals and autocorrelation function of residuals are plotted for $\delta = 1/2$.

is 0.025). Statistical noise, added to $g(t)$, $f(t)$, $f_{\|}(t)$ and $f_{\perp}(t)$ is described by Poisson statistics: the number of counts in every channel is the Poisson random value with the mean equal to the exact value in that channel. The number of counts in the peak channel is set to 10^4 for $g(t)$, $f(t)$ or $f_{\|}(t)$ (the peak channel for $f_{\perp}(t)$ is calculated according to Eqs. (22) and (23)). In every simulation experiment, the estimation was repeated for 100 runs of the generated fluorescence and instrumental functions, each one with a different realization of statistical noise. The estimators are stored for the calculation of mean value:

$$M\{p_k\} = \sum_{i=0}^{100} {}^{i}p_k/100, \tag{25}$$

and variance:

$$\sigma^2\{p_k\} = \sum_{i=0}^{100} {}^{i}p_k^2/100 - M\{p_k\}^2, \tag{26}$$

where ${}^{i}p_k$ is the estimator for the kth parameter, obtained after the ith run.

Tables 1–3 present the dependence of the fitting accuracy on the dimensional parameter δ. Four values of dimensional parameter were used: 0.75 ('fractal' dimension [8]), $1/2$ (three dimensions), $1/3$ (two dimensions) and $1/6$ (single dimension). Typical results of the simulation and subsequent fit in terms of single stretched exponential for fluorescence (Eq. (1)) and for anisotropy (Eq. (16) with $a_2 = 0$) are presented in Figs. 1 and 2, respectively, for four values of the dimensional parameter δ. Residuals and autocorrelation functions are plotted for $\delta = 1/2$. Fitted values of the parameters of stretch exponential decay were used as initial guesses for Marquardt non-linear method of least squares (MNLLS), described in detail elsewhere [10,18]. The mean values and standard deviations of the estimators obtained by MNLLS are also presented in the tables for comparison. Numerical experiments show

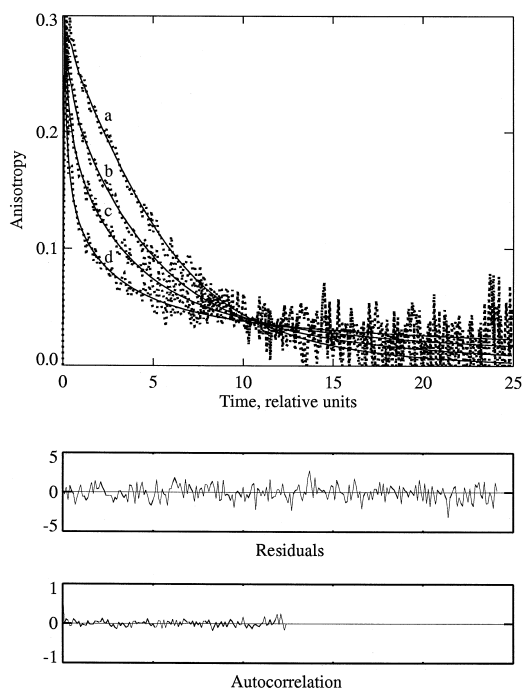

Fig. 2. Simulated (dots) and fitted (smooth curve) anisotropy stretched exponential decay (Eq. (17)) for four values of the dimensional parameter δ: 0.75 (a), $1/2$ (b), $1/3$ (c) and $1/6$ (d). Residuals and autocorrelation function of residuals are plotted for $\delta = 1/2$.

that MNLLS normally ensures less biased estimators, especially for smaller dimension parameters δ ($\delta = 1/3,\ 1/6$), as well as lower values of standard deviations.

Table 1 contains the results of the restoration of stretched exponential decay Eq. (1). Eq. (6) is used for the estimation of the decay time β (column 3 for the undistorted decay and column 6 for the convoluted decay) and of the energy transfer parameter C (column 4 for the undistorted decay and column 7 for the convoluted decay), provided δ is fixed to the true value. The dimensional parameter δ (column 5 for the undistorted decay and column 8 for the convoluted decay) was fitted separately according to Eq. (9). This algorithm requires an increased number of time channels (up to 1024) to allow good resolution. It should be noted that deconvolution in this case does not significantly influence the accuracy of fit.

The advantage of the proposed algorithm is demonstrated in Fig. 3 by the dependence of the convergence time of MNLLS with the manually chosen initial guesses related to the convergence times of MNLLS with the initial guesses, obtained by the linear algorithm. The improvement is especially noticeable for the curves with instrumental response, when one needs to calculate convolution several times on each iteration. Good initial guesses, decreasing the number of iterations, also decrease computational costs.

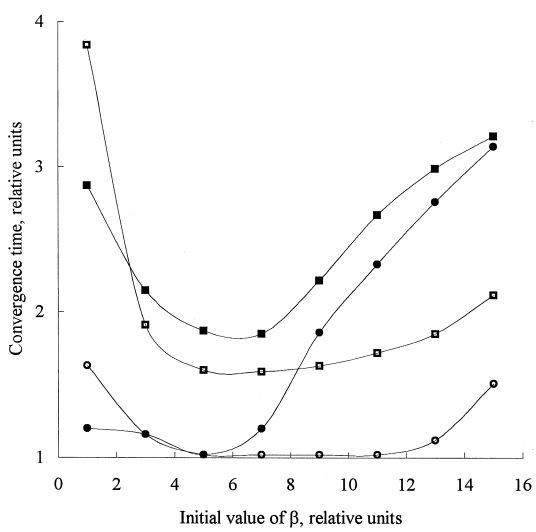

Fig. 3. Dependence of the convergence time of MNLLS with the manually chosen initial guesses ($C = 0.5,\ \delta = 0.5$ (empty points) and $C = 2.0,\ \delta = 0.5$ (filled points)) related to the convergence times of MNLLS with the initial guesses, obtained by the proposed algorithm, on the initial guess for the decay time β, for stretched exponential decay (1), accounting instrumental response (squares) and without instrumental response (rounds). True values of parameters are: $\beta = 8.0,\ C = 1.0$ and $\delta = 0.5$ (all values are given in relative units).

Analysis of the intensity decay Eq. (12) was based on the analytical solution of the set Eq. (16) of algebraic equations. Results are presented in Table 2 for four fixed values of δ. One can see that the decay with the smallest values of δ is the most troublesome. The bias and variance, increases when δ tends to reach the lowest value. In order to have reasonable resolution for $\delta = 1/6$, one has even to increase the number of time channels up to 1024. This effect can be explained by strong coupling between the parameters of the stretched exponential decay, which sharply increases for the lowest value of the dimensional parameter.

Table 3 contains the results of estimation of the anisotropy decay parameters, represented by Eq. (18). Analysis was performed according to Eq. (19). Two cases were explored: stretched exponential with a time-independent component ($a_2 = 0.1$) and without time-independent component ($a_2 = 0$). Results show that the time-independent component can be extracted more or less confidently under the present conditions, despite the fact that the correlation between the energy transfer parameter γ and amplitude a_2 is very high. The latter is particularly seen for the decays with the lowest value of the dimensional parameter.

Simulation experiments prove that the proposed algorithms are suitable for the preliminary analysis of a broad range of fluorescence decay models based on stretched exponential decay law, ensuring reasonable estimators for the parameters in most cases and providing higher performance of the subsequent fitting by MNLLS.

7. Experimental data

The presented algorithms were applied to fit the experimentally obtained fluorescence and anisotropy decays of dimethylaminonitrostilbene (DANS)

Table 4
Estimated fluorescence and anisotropy parameters of DANS in PMMA film

	Fluorescence				Anisotropy			
Estimator	I_0	β	C	A	a_1	C	a_2	χ^2
Linear	0.57	3.20	1.29	0.43	0.12	0.87	0.088	1.32
MNLLS	0.63	3.10	1.17	0.37	0.15	0.60	0.045	1.21
Left	0.53	2.55	0.98	0.33	0.09	0.30	0.00	1.35
Right	0.74	3.81	1.35	0.48	0.19	1.29	0.10	1.35

Confidence intervals (Left and Right bounds) for the parameters at 67% level are given for MNLLS.

molecules dissolved in polymethyl methacrylate (PMMA) film. We consider this substance as having three dimensions ($\delta = 0.5$), as the thickness of PMMA film is much larger than the molecular size of DANS. Experimental decays have 1024 data points and the resolution per data point is 10 ps. The instrumental response function for deconvolution was obtained using a scattering solution. The details of the experimental set-up used for the polarized fluorescence decay measurements and sample preparation have been described elsewhere [19].

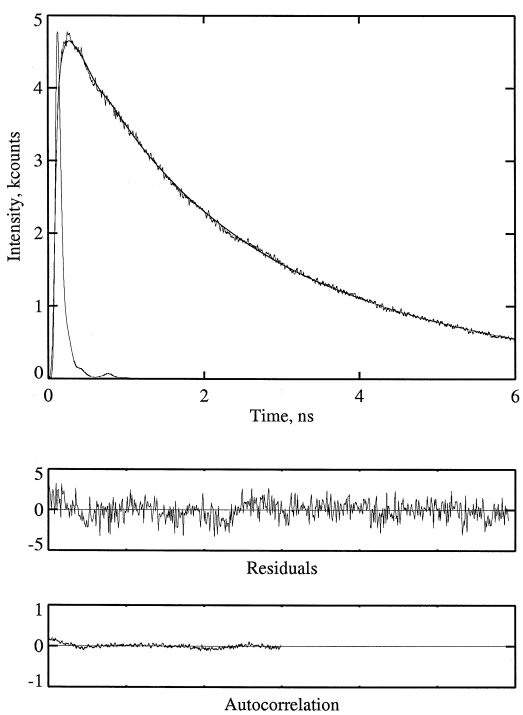

Fig. 4. Experimental (noisy curve) fluorescence decay of DANS in PMMA film and decay fitted (smooth curve) by stretched exponential decay law (Eq. (12)). Instrumental function (the narrowest curve) was normalized to the maximum of fluorescence curve.

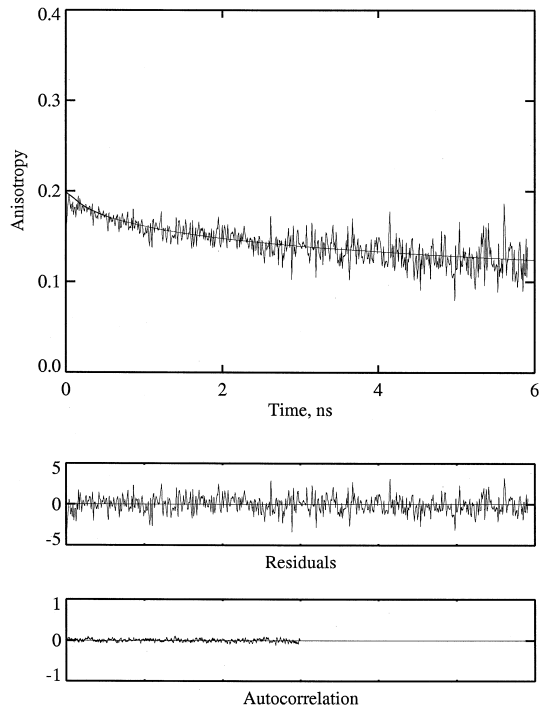

Fig. 5. Experimental (noisy curve) anisotropy decay of DANS in PMMA film and decay fitted (smooth curve) by stretched exponential decay law (Eq. (18)).

The results of the fit (for the sample excited at 527 nm and detected at 580 nm) are given in Table 4. Eq. (12) was used for the approximation of the fluorescence decay of DANS in PMMA (containing 10 wt.% DANS). Anisotropy analysis was done in terms of Eq. (18). The goodness of fit was judged by the χ^2 criterion and by the autocorrelation function of residuals [18]. The error estimation of the recovered parameters was performed by the exhaustive search method [20]. Typical results of the deconvolution for the fluorescence and anisotropy decays of DANS in PMMA film are presented in Figs. 4 and 5, respectively.

Table 4 shows that, although MNLLS undoubtedly improves the total fit quality (expressed in

lower values of χ^2 criterion), in all cases the parameters, predicted according to the proposed algorithms, are already reasonably good and fall within the parameter confidence interval obtained by MNLLS. Having such initial guesses, MNLLS often needs just a couple of iterations to find χ^2 minima. For that reason, the proposed algorithms lead to a considerable improvement in performance the fluorescence decay analysis software.

References

[1] J.N. Demas, Excited State Lifetime Measurements, Academic Press, New York, 1983.
[2] D.V. O'Connor, D. Phillips, Time Correlated Single Photon Counting, Academic Press, London, 1984.
[3] G.H. Fredrickson, C.W. Frank, Macromolecules 16 (1983) 1198.
[4] K.P. Ghiggino, T.A. Smith, Prog. React. Kinet. 18 (1993) 375.
[5] J.W. Hofstraat, H.J. Verhey, J.W. Verhoeven, M.U. Kumke, G. Li, S.L. Hemmingsen, L.B. McGown, Polymer, in press.
[6] T. Förster, Z. Naturforsch 4a (1949) 321.
[7] M. Van der Auweraer, P. Ballet, F.C. De Schryver, A. Kowalczyk, Chem. Phys. 187 (1994) 399.
[8] P. Lianos, G. Duportail, Biophys. Chem. 48 (1993) 293.
[9] J.C. Love, J.N. Demas, Rev. Sci. Instrum. 54 (1983) 1787.
[10] P.R. Bevington, Data Reduction and Error Analysis for the Physical Sciences, McGraw-Hill, New York, 1969.
[11] I. Yamazaki, N. Tamai, T. Yamazaki, J. Phys. Chem. 94 (1990) 516.
[12] K.A. Peterson, M.B. Zimmt, S. Linse, R.P. Domingue, M.D. Fayer, Macromolecules 20 (1987) 168.
[13] C.R. Gochanour, M.D. Fayer, J. Phys. Chem. 85 (1981) 1989.
[14] J. Lakowicz, Principles of Fluorescence Spectroscopy, Plenum Press, New York, 1983.
[15] V.V. Apanasovich, E.G. Novikov, Opt. Commun. 78 (1990) 279.
[16] S. Hirayama, Y. Sakai, K.P. Ghiggino, T.A. Smith, J. Photochem. Photobiol., A 52 (1990) 27.
[17] A. van Hoek, K. Vos, A.J.W.G. Visser, IEEE J. Quantum Electron. 23 (1987) 1812.
[18] A. Grinvald, I. Steinberg, Anal. Biochem. 59 (1979) 583.
[19] E.G. Novikov, A. van Hoek, A.J.W.G. Visser, J.W. Hofstraat, in preparation.
[20] J.M. Beechem, E. Gratton, M. Ameloot, J.R. Knutson, L. Brand, in: J.R. Lakowicz (Ed.), Topics in Fluorescence Spectroscopy, vol. 2, Plenum Press, New York, 1991, p. 241.